

Upper limit on the flux of photons with energies above 10^{19} eV using the Telescope Array surface detector

T. Abu-Zayyad,¹ R. Aida,² M. Allen,¹ R. Anderson,¹ R. Azuma,³ E. Barcikowski,¹ J.W. Belz,¹ D.R. Bergman,¹ S.A. Blake,¹ R. Cady,¹ B.G. Cheon,⁴ J. Chiba,⁵ M. Chikawa,⁶ E.J. Cho,⁴ W.R. Cho,⁷ H. Fujii,⁸ T. Fujii,⁹ T. Fukuda,³ M. Fukushima,^{10,11} D. Gorbunov,¹² W. Hanlon,¹ K. Hayashi,³ Y. Hayashi,⁹ N. Hayashida,¹⁰ K. Hibino,¹³ K. Hiyama,¹⁰ K. Honda,² T. Iguchi,³ D. Ikeda,¹⁰ K. Ikuta,² N. Inoue,¹⁴ T. Ishii,² R. Ishimori,³ D. Ivanov,^{1,15} S. Iwamoto,² C.C.H. Jui,¹ K. Kadota,¹⁶ F. Kakimoto,³ O. Kalashev,¹² T. Kanbe,² K. Kasahara,¹⁷ H. Kawai,¹⁸ S. Kawakami,⁹ S. Kawana,¹⁴ E. Kido,¹⁰ H.B. Kim,⁴ H.K. Kim,⁷ J.H. Kim,¹ J.H. Kim,⁴ K. Kitamoto,⁶ S. Kitamura,³ Y. Kitamura,³ K. Kobayashi,⁵ Y. Kobayashi,³ Y. Kondo,¹⁰ K. Kuramoto,⁹ V. Kuzmin,¹² Y.J. Kwon,⁷ J. Lan,¹ S.I. Lim,¹⁹ S. Machida,³ K. Martens,¹¹ T. Matsuda,⁸ T. Matsuura,³ T. Matsuyama,⁹ J.N. Matthews,¹ M. Minamino,⁹ K. Miyata,⁵ Y. Murano,³ I. Myers,¹ K. Nagasawa,¹⁴ S. Nagataki,²⁰ T. Nakamura,²¹ S.W. Nam,¹⁹ T. Nonaka,¹⁰ S. Ogio,⁹ M. Ohnishi,¹⁰ H. Ohoka,¹⁰ K. Oki,¹⁰ D. Oku,² T. Okuda,²² A. Oshima,⁹ S. Ozawa,¹⁷ I.H. Park,¹⁹ M.S. Pshirkov,^{12,23} D.C. Rodriguez,¹ S.Y. Roh,²⁴ G.I. Rubtsov,¹² D. Ryu,²⁴ H. Sagawa,¹⁰ N. Sakurai,⁹ A.L. Sampson,¹ L.M. Scott,¹⁵ P.D. Shah,¹ F. Shibata,² T. Shibata,¹⁰ H. Shimodaira,¹⁰ B.K. Shin,⁴ J.I. Shin,⁷ T. Shirahama,¹⁴ J.D. Smith,¹ P. Sokolsky,¹ B.T. Stokes,¹ S.R. Stratton,^{1,15} T. Stroman,¹ S. Suzuki,⁸ Y. Takahashi,¹⁰ M. Takeda,¹⁰ A. Taketa,²⁵ M. Takita,¹⁰ Y. Tameda,¹⁰ H. Tanaka,⁹ K. Tanaka,²⁶ M. Tanaka,⁹ S.B. Thomas,¹ G.B. Thomson,¹ P. Tinyakov,^{12,23} I. Tkachev,¹² H. Tokuno,³ T. Tomida,²⁷ S. Troitsky,¹² Y. Tsunesada,³ K. Tsutsumi,³ Y. Tsuyuguchi,² Y. Uchihori,²⁸ S. Udo,¹³ H. Ukai,² G. Vasiloff,¹ Y. Wada,¹⁴ T. Wong,¹ M. Wood,¹ Y. Yamakawa,¹⁰ R. Yamane,⁹ H. Yamaoka,⁸ K. Yamazaki,⁹ J. Yang,¹⁹ Y. Yoneda,⁹ S. Yoshida,¹⁸ H. Yoshii,²⁹ X. Zhou,⁶ R. Zollinger,¹ and Z. Zundel¹

(Telescope Array Collaboration)

¹High Energy Astrophysics Institute and Department of Physics and Astronomy, University of Utah, Salt Lake City, Utah, USA

²University of Yamanashi, Interdisciplinary Graduate School of Medicine and Engineering, Kofu, Yamanashi, Japan

³Graduate School of Science and Engineering, Tokyo Institute of Technology, Meguro, Tokyo, Japan

⁴Department of Physics and The Research Institute of Natural Science, Hanyang University, Seongdong-gu, Seoul, Korea

⁵Department of Physics, Tokyo University of Science, Noda, Chiba, Japan

⁶Department of Physics, Kinki University, Higashi Osaka, Osaka, Japan

⁷Department of Physics, Yonsei University, Seodaemun-gu, Seoul, Korea

⁸Institute of Particle and Nuclear Studies, KEK, Tsukuba, Ibaraki, Japan

⁹Graduate School of Science, Osaka City University, Osaka, Osaka, Japan

¹⁰Institute for Cosmic Ray Research, University of Tokyo, Kashiwa, Chiba, Japan

¹¹Kavli Institute for the Physics and Mathematics of the Universe, University of Tokyo, Kashiwa, Chiba, Japan

¹²Institute for Nuclear Research of the Russian Academy of Sciences, Moscow, Russia

¹³Faculty of Engineering, Kanagawa University, Yokohama, Kanagawa, Japan

¹⁴The Graduate School of Science and Engineering, Saitama University, Saitama, Saitama, Japan

¹⁵Department of Physics and Astronomy, Rutgers University, Piscataway, USA

¹⁶Department of Physics, Tokyo City University, Setagaya-ku, Tokyo, Japan

¹⁷Advanced Research Institute for Science and Engineering, Waseda University, Shinjuku-ku, Tokyo, Japan

¹⁸Department of Physics, Chiba University, Chiba, Chiba, Japan

¹⁹Department of Physics and Institute for the Early Universe, Ewha Womans University, Seodaemun-gu, Seoul, Korea

²⁰Yukawa Institute for Theoretical Physics, Kyoto University, Sakyo, Kyoto, Japan

²¹Faculty of Science, Kochi University, Kochi, Kochi, Japan

²²Department of Physical Sciences, Ritsumeikan University, Kusatsu, Shiga, Japan

²³Service de Physique Théorique, Université Libre de Bruxelles, Brussels, Belgium

²⁴Department of Astronomy and Space Science, Chungnam National University, Yuseong-gu, Daejeon, Korea

²⁵Earthquake Research Institute, University of Tokyo, Bunkyo-ku, Tokyo, Japan

²⁶Department of Physics, Hiroshima City University, Hiroshima, Hiroshima, Japan

²⁷RIKEN, Advanced Science Institute, Wako, Saitama, Japan

²⁸National Institute of Radiological Science, Chiba, Chiba, Japan

²⁹Department of Physics, Ehime University, Matsuyama, Ehime, Japan

We search for ultra-high energy photons by analyzing geometrical properties of shower fronts of events registered by the Telescope Array surface detector. By making use of an event-by-event statistical method, we derive upper limits on the absolute flux of primary photons with energies above 10^{19} , $10^{19.5}$ and 10^{20} eV based on the first three years of data taken.

I. INTRODUCTION

The Telescope Array (TA) experiment [1] is a hybrid ultra-high energy (UHE) cosmic ray detector covering about 700 km^2 in central Utah, USA. It is composed of a Surface Detector (SD) array and three Fluorescence Detector (FD) stations. The TA SD array consists of 507 plastic scintillator detectors on a square grid with 1.2 km spacing [2]. They each contain two layers of 1.2 cm thick plastic scintillator 3 m^2 in area. The three FD stations [3] contain a total of 38 telescopes overlooking the air space above the array of scintillator detectors. The purpose of this paper is to present the photon search capabilities of the Telescope Array surface detector and to search for primary photons in the cosmic ray flux. We place the limits on the integral flux of photons for energies greater than E_0 , where E_0 takes values 10^{19} , $10^{19.5}$ and 10^{20} eV.

At present there is no experimental evidence for primary UHE photons. However, several limits on the photon flux have been set by independent experiments. These include Haverah Park [4], AGASA [5], Yakutsk [6, 7] (see also reanalyses of the AGASA [8] and AGASA+Yakutsk [9] data at energies greater than 10^{20} eV) and the Pierre Auger Observatory [10–12].

Photon limits may be used to constrain the parameters of top-down models [13]. The photon searches may be used to assess parameters of astrophysical sources in the Greisen-Zatsepin-Kuzmin [14, 15] cut-off scenario which predicts photons as ever present secondaries. If UHE photons are observed, they will be a supporting evidence for the GZK nature of the spectrum break at the highest energies observed by HiRes [16], Pierre Auger Observatory [17] and TA [18]. Photon flux is sensitive to the mass composition of cosmic rays and hence may be used as a probe of the latter [19, 20]. The results of the photon search also constrain parameters of Lorentz invariance violation [21–25]. Finally, photons with energies greater than $\sim 10^{18}$ eV could be responsible for CR events correlated with BL Lac type objects on an angular scale significantly smaller than the expected deflection for protons in cosmic magnetic fields. This suggests neutral primaries [26, 27] (see Ref. [28] for a possible mechanism).

Since the TA detectors are composed of thin scintillators, they respond equally to the muon and electromagnetic components of the extensive air shower and are therefore sensitive to showers induced by photon primaries (see e.g. Ref. [29] for discussion). We use the shower front curvature as a Composition-sensitive parameter (C-observable) and a modification of an event-by-event statistical method [30] to constrain the photon integral flux above the given energy. For the Energy-sensitive parameter (E-observable), we use the scintillator signal density at 800 m core distance $\mathcal{S} \equiv S_{800}$. The comparison of an event-by-event statistical method with the “photon median” method [11] is presented.

hadron-induced EAS gamma-induced EAS

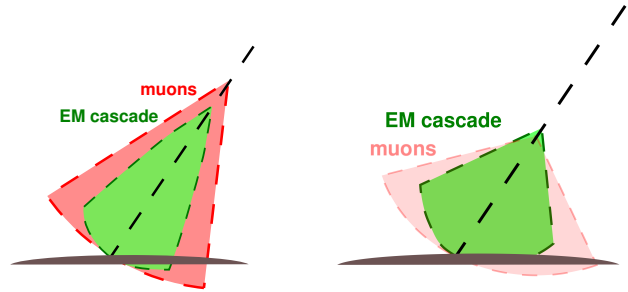


FIG. 1: Illustrative view of hadron- (left) and gamma-induced (right) showers. Gamma-induced shower is deeper due to smaller cross-section of the first interaction. Moreover, the hadronic cascade is secondary with respect to electromagnetic in photon-induced showers. The latter contains fewer muons (shown in red) and have larger curvature of the shower front.

II. SIMULATIONS

Extensive Air Showers (EAS) induced by photon primaries differ significantly from hadron-induced events (see e.g. [31] for a review). Photon induced showers contain fewer muons and have a deeper shower maximum when compared to hadronic showers. The latter results in the shower front having more curvature at the surface as illustrated in Figure 1. At the highest energies, there are two competing effects responsible for the diversity of showers induced by photon primaries. First, the electromagnetic cross-section is suppressed at energies, $E > 10^{19}$ eV due to the Landau, Pomeranchuk [32] and Migdal [33] (LPM) effect. The LPM effect delays the first interaction so that the shower arrives at ground level underdeveloped. The second effect is e^\pm pair production which is due to photon interaction with the geomagnetic field above the atmosphere. Secondary electrons produce gamma rays by synchrotron radiation generating a cascade in the geomagnetic field. The probability of photon conversion is a function of photon energy and the perpendicular component of geomagnetic field [34]. The shower development therefore depends on both the zenith and azimuthal angles of the photon arrival direction.

The event-by-event method [30] requires a set of simulated photon-induced showers for the analysis of each real shower. We simulate the library of these showers with different primary energies and arrival directions. For the highest energy candidates (events which may be induced by a photon with primary energy greater than $10^{19.5}$ eV) we simulate individual sets of showers with fixed zenith and azimuthal angles. At these energies, the shower development becomes azimuth-angle dependent due to the photon cascading in the geomagnetic field [31].

We use CORSIKA [35] with EGS4 [36] to model

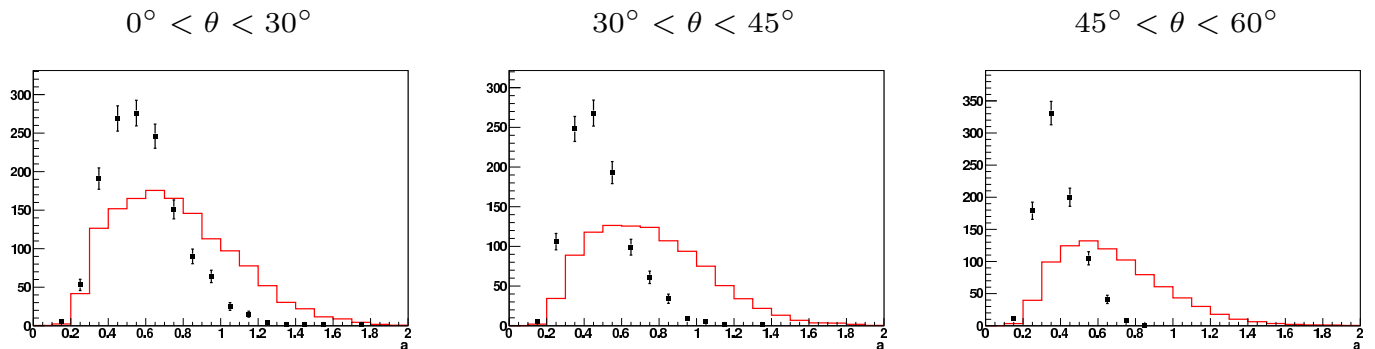


FIG. 2: Linsley curvature parameter distribution for three different zenith angle regions for reconstructed $E_\gamma > 10^{19}$ eV. The black points refer to data, red line represents the photon MC generated with an E^{-2} spectrum.

the electromagnetic interactions and PRESHOWER code [37] for geomagnetic interactions. There is no significant dependence on the hadronic model because only photon-induced simulated showers are used in the method. The showers are simulated with thinning and the dethinning procedure is adopted [38] to simulate realistic shower fluctuations.

The detector response is accounted for by using lookup tables generated by GEANT4 [39] simulations. Real-time array status and detector calibration information are used for each Monte Carlo (MC) simulated event. The Monte-Carlo events are recorded in the same format as real events and analysis procedures are applied in the same way to both. The photon-induced MC set contains 2×10^6 triggered events produced from 3380 CORSIKA showers by randomizing core location [40].

III. DATA SET

We use the Telescope Array surface detector data set observed and recorded between 2008-05-11 and 2011-05-01. During this time period, the surface detector array was collecting data with a duty cycle greater than 95% [2].

We reconstruct each event with a joint fit of the geometry and Lateral Distribution Function (LDF) and determine the Linsley curvature parameter “ a ” (see Appendix A for definition) along with the arrival direction, core location, and signal density at 800 meters $\mathcal{S} \equiv S_{800}$. As noted above, the same reconstruction procedure is applied to both data and Monte-Carlo events.

For each real event, “ i ”, we estimate the energy of the hypothetical photon primary, $E_\gamma^i = E_\gamma(\mathcal{S}^i, \theta^i, \phi^i)$, i.e. the average energy of the primary photon, inducing the shower with the same arrival direction and \mathcal{S} . The look-up table for $E_\gamma(\mathcal{S}, \theta, \phi)$ is built using the photon MC set; the dependence on azimuthal angle, ϕ , is relevant for events with $E_\gamma > 10^{19.5}$ eV where geomagnetic preshowering is substantial. Photon-induced showers are naturally highly fluctuating. Consequently, the accuracy of the determination of E_γ is about 50% at the one sigma

level. In the present analysis, E_γ is used for event selection only and therefore its fluctuations are well accounted for in the exposure calculation. The effect of these fluctuations is “lost” photons [30], i.e. the photons with reconstructed energy below the energy cut. This will be estimated in Section V.

We imposed the following requirements on both the data and MC events:

1. The shower core is inside the array boundary with the distance to the boundary larger than 1200 m;
2. Zenith angle cut: $45^\circ < \theta < 60^\circ$;
3. The number of scintillator detectors triggered is ≥ 7 ;
4. The joint fit quality cut, $\chi^2/\text{d.o.f.} < 5$;
5. \mathcal{S} cut: $E_\gamma(\mathcal{S}_{obs}^i, \theta^i, \phi^i) > 10^{19}$ eV or $E_\gamma > 10^{19.5}$ eV depending on the energy region discussed (the second variant is used for both $E_0 = 10^{19.5}$ and $E_0 = 10^{20}$ eV).

The cuts determine a photon detection efficiency which is greater than 50% for showers induced by primary photons with energy above 10^{19} eV. The calculation of exposure is given in Section V. The resulting data set contains 877 events with $E_\gamma > 10^{19}$ eV and $45^\circ < \theta < 60^\circ$ which we used for our photon search.

IV. METHOD

To estimate the flux limit, we used an event-by-event method [30]. The Linsley curvature parameter “ a ” is used as a C-observable and $\mathcal{S} \equiv S_{800}$ is used as an E-observable. For each real event, “ i ”, we estimate the pair of parameters $(\mathcal{S}_{obs}^i, a_{obs}^i)$ and the arrival direction (θ^i, ϕ^i) from the fit of shower front geometry and LDF. Histograms of Linsley curvature are shown in Figure 2. Note that both data and MC distributions show smallest variance in the region $45^\circ < \theta < 60^\circ$. The latter motivates the selection of zenith angle range for the further procedure.

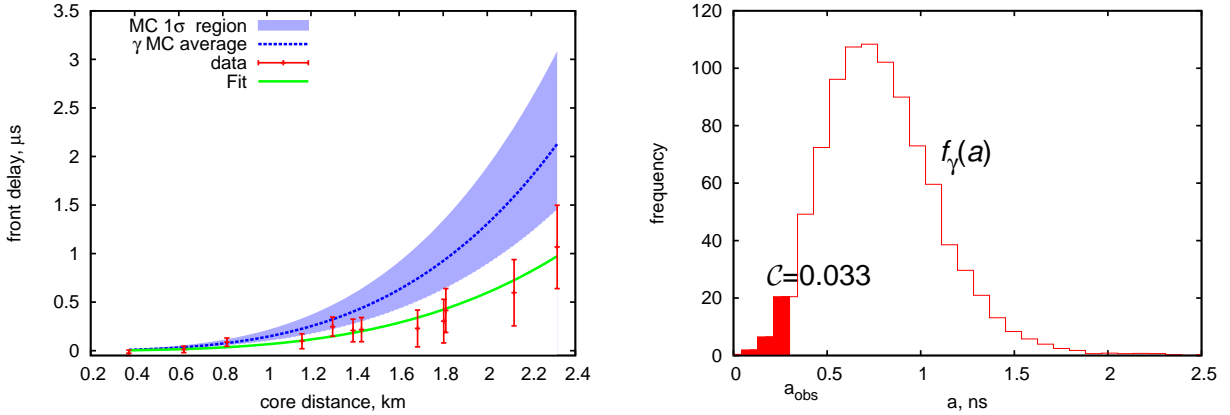


FIG. 3: Left: Fit of the shower front for an event (2008-08-13 14:02:01, $\theta = 53.6^\circ$, $E_\gamma = 1.29 \times 10^{19}$ eV, $C=0.033$) compared to average over all photon MC events with the same zenith angle and \mathcal{S} . 68% of MC events have a shower front delay within the shaded 1σ region. The front delay is counted from the plane front arrival time. Right: $f_\gamma(a)$ for the same event; a_{obs} – observed value of curvature. The filled region indicates MC events with curvature smaller than a_{obs} (3.3% of MC events).

We selected simulated gamma-induced showers compatible with the observed θ^i , ϕ^i and \mathcal{S}_{obs}^i and calculate the curvature distribution of the simulated photon showers, $f_\gamma^i(a)$, as discussed in Reference [30]. For each event, we determined the percentile rank of Linsley parameter, a , for photon primaries

$$\mathcal{C}^i = \int_{-\infty}^{a_{obs}^i} f_\gamma^i(a) da,$$

which is the value of the integral probability distribution function at the observed curvature. The shower front fit, $f_\gamma(a)$, and \mathcal{C} for one of the events is shown in Figure 3.

The distribution of \mathcal{C} for the data and MC is shown in Figure 4. Although the distribution of $f_\gamma^i(a)$ varies with energy and arrival direction, \mathcal{C}^i for gamma-ray primaries would be distributed between 0 and 1 uniformly by definition [43]. On the other hand, the actual distribution of \mathcal{C}^i in the data is strongly non-uniform (most of the events have \mathcal{C}^i below 0.5).

Since the simulations of hadron-induced showers depend strongly on the hadronic interaction model, we do not use the hadronic showers simulations in calculation of the photon limit.

Suppose that the integral flux of primary photons over a given energy range is F_γ . Then we expect to detect

$$\bar{n}(F_\gamma) = (1 - \lambda)F_\gamma A_{geom} \quad (1)$$

photon events on average, where A_{geom} is the geometrical exposure of the experiment for a given data set and λ is the fraction of “lost” photons (i.e. photons with primary energies within the interesting region which failed to enter the data set due to triggering efficiency and cuts).

We calculate an upper limit on the primary photon flux based on the idea that photons satisfy a uniform distribution from 0 to 1 of the variable \mathcal{C} . To do this, we examine

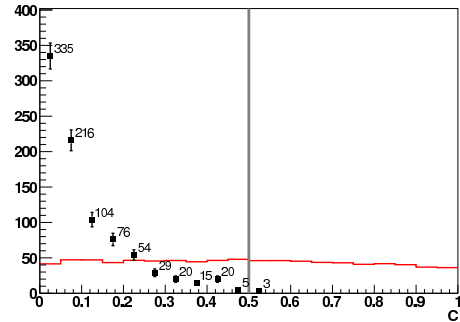


FIG. 4: \mathcal{C} distribution for the data set $E_\gamma > 10^{19}$ eV, $45^\circ < \theta < 60^\circ$. The black points show the data and the red line indicates the photon MC generated with an E^{-2} spectrum. The MC photon median is represented by the vertical gray line.

all possible combinations of n events from the data set, where n covers the range from 3 to some large value M . We compare each combination to a uniform \mathcal{C} distribution using the Smirnov-Cramer-von Mises test [41], and let $\mathcal{P}(n)$ be the largest probability found in this way. By definition of the test $\mathcal{P}(0) \equiv \mathcal{P}(1) \equiv \mathcal{P}(2) \equiv 1$ and we assume $M = 100$ (for which all probabilities vanish in the considered cases). See Appendix B for a description of the Smirnov-Cramer-von Mises test. To constrain the flux F_γ at the confidence level ξ , we require

$$\sum_{n=0}^M \mathcal{P}(n)W(n, \bar{n}(F_\gamma)) < 1 - \xi, \quad (2)$$

where $W(n, \bar{n})$ is the Poisson probability of finding n events when the mean is \bar{n} . To constrain the flux at the 95% confidence level (CL) we set $\xi = 0.95$ and find \bar{n} from equation (2). The upper limit on the flux follows

Cut	E_0 , eV		
	10^{19}	$10^{19.5}$	10^{20}
$n_{det} \geq 7$	72%	94%	97%
$\chi^2/\text{d.o.f.} < 5$	68%	89%	95%
\mathcal{S} cut	57%	70%	95%
Total:	57%	70%	95%

TABLE I: Relative exposure of TA SD ($1 - \lambda$) to photons after consecutive application of the cuts.

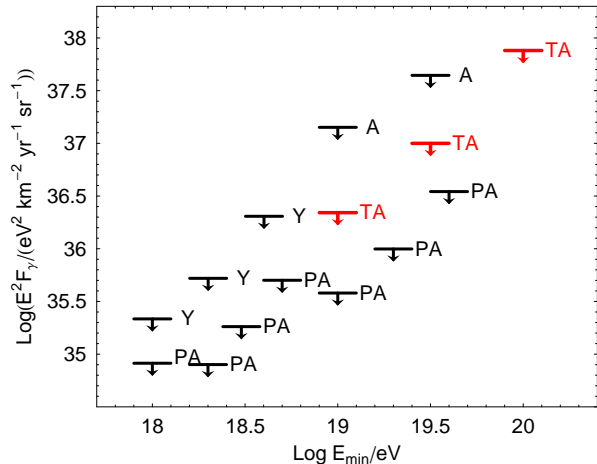


FIG. 5: Photon flux limits of the present work (TA) compared to the previous limits by AGASA (A) [5], Yakutsk (Y) [7] and Pierre Auger Observatory (PA) [11, 12].

from equations (1),

$$F_\gamma < \frac{\bar{n}}{(1 - \lambda)A_{geom}}. \quad (3)$$

This method does not require any assumptions about hadron-induced showers and does not require the C-observable to be strongly discriminating (like the muon density used in [6, 7, 9]).

V. EXPOSURE

The geometrical exposure for the SD observation period with $45^\circ < \theta < 60^\circ$ and boundary cut is

$$A_{geom} = 1286 \text{ km}^2 \text{ sr yr}. \quad (4)$$

The fraction of “lost” photons is calculated using a photon MC set generated with an E^{-2} spectrum. The values of $(1 - \lambda)$ after consecutive application of cuts are shown in Table I.

VI. RESULTS

Using the statistical method (Section IV) we arrive at the following results:

$$\begin{aligned} \bar{n} &< 14.1 \text{ (95\% CL)}, E_\gamma > 10^{19} \text{ eV}, \\ \bar{n} &< 8.7 \text{ (95\% CL)}, E_\gamma > 10^{19.5} \text{ eV}, \\ \bar{n} &< 8.7 \text{ (95\% CL)}, E_\gamma > 10^{20} \text{ eV}. \end{aligned}$$

$$\begin{aligned} F_\gamma &< 1.9 \times 10^{-2} \text{ km}^{-2} \text{ sr}^{-1} \text{ yr}^{-1} \text{ (95\% CL)}, E_\gamma > 10^{19} \text{ eV}, \\ F_\gamma &< 0.97 \times 10^{-2} \text{ km}^{-2} \text{ sr}^{-1} \text{ yr}^{-1} \text{ (95\% CL)}, E_\gamma > 10^{19.5} \text{ eV}, \\ F_\gamma &< 0.71 \times 10^{-2} \text{ km}^{-2} \text{ sr}^{-1} \text{ yr}^{-1} \text{ (95\% CL)}, E_\gamma > 10^{20} \text{ eV}. \end{aligned}$$

These photon limits are shown along with the results of the other experiments in Figure 5.

We obtain photon fraction limits by dividing the corresponding flux limits by the integral flux of the Telescope Array SD spectrum [18]:

$$\begin{aligned} \varepsilon_\gamma &< 6.2\% \text{ (95\% CL)}, E_\gamma > 10^{19} \text{ eV}, \\ \varepsilon_\gamma &< 28.5\% \text{ (95\% CL)}, E_\gamma > 10^{19.5} \text{ eV}. \end{aligned}$$

The limits strongly constrain the top-down models of the origin of cosmic rays, see [42] for discussion.

Next, we compare the results of the event-by-event method with the results of the simpler “photon median” method [11]. In the latter, the events having curvature greater than the median photon curvature are identified as photon candidates. This criteria corresponds to $\mathcal{C} > 0.5$. We observe three candidate events with energy greater than 10^{19} eV (see Figure 4) and no candidate events above $10^{19.5}$ eV. This corresponds to a 95% Poisson confidence limit of $\bar{n}/2 < 8.25$ and $\bar{n}/2 < 3.09$. The flux limits are $F_\gamma < 2.3 \times 10^{-2}$, $F_\gamma < 0.69 \times 10^{-2}$ and $F_\gamma < 0.51 \times 10^{-2} \text{ km}^{-2} \text{ sr}^{-1} \text{ yr}^{-1}$ for $E_0 = 10^{19}$, $10^{19.5}$ and 10^{20} eV correspondingly. The limits using the two methods are in mutual agreement.

Finally we discuss how the result depends on the assumption of the E^{-2} primary photon spectrum. We repeated the analysis with varied spectral index and for $E > 10^{19}$ eV arrived at $F_\gamma < 2.2 \times 10^{-2}$ and $F_\gamma < 1.8 \times 10^{-2} \text{ km}^{-2} \text{ sr}^{-1} \text{ yr}^{-1}$ for $E^{-1.5}$ and $E^{-2.5}$ primary spectra correspondingly. The limits for energy greater than $10^{19.5}$ and 10^{20} eV are less sensitive to the spectral assumption.

Both the use of plastic scintillators sensitive to photon-induced showers and the application of event-by-event statistical method allowed us to put stringent limits on the flux of primary photons with energies in excess of 10^{19} eV with the data obtained during three years of the TA surface detector operation. The photons propagate without deflection by magnetic fields and therefore in the case of the few nearby sources we may not expect an isotropic flux. It worth mentioning that the limits of this paper are strongest among those obtained in the northern hemisphere. The result depends neither on the choice of hadronic interaction model, nor on possible systematics in the energy determination of hadronic primaries.

Acknowledgments

The Telescope Array experiment is supported by the Japan Society for the Promotion of Science through Grants-in-Aids for Scientific Research on Specially Promoted Research (21000002) “Extreme Phenomena in the Universe Explored by Highest Energy Cosmic Rays” and for Scientific Research (19104006), and the Inter-University Research Program of the Institute for Cosmic Ray Research; by the U.S. National Science Foundation awards PHY-0307098, PHY-0601915, PHY-0649681, PHY-0703893, PHY-0758342, PHY-0848320, PHY-1069280, and PHY-1069286; by the National Research Foundation of Korea (2007-0093860, R32-10130, 2012R1A1A2008381, 2013004883); by the Russian Academy of Sciences, by the grant of the President of the Russian Federation MK-1170.2013.2, Dynasty Foundation, RFBR grants 11-02-01528, 13-02-01311 and 13-02-01293 (INR), IISN project No. 4.4509.10 and Belgian Science Policy under IUAP VII/37 (ULB). The foundations of Dr. Ezekiel R. and Edna Wattis Dumke, Willard L. Eccles and the George S. and Dolores Dore Eccles all helped with generous donations. The State of Utah supported the project through its Economic Development Board, and the University of Utah through the Office of the Vice President for Research. The experimental site became available through the cooperation of the Utah School and Institutional Trust Lands Administration (SITLA), U.S. Bureau of Land Management, and the U.S. Air Force. We also wish to thank the people and the officials of Millard County, Utah for their steadfast and warm support. We gratefully acknowledge the contributions from the technical staffs of our home institutions. An allocation of computer time from the Center for High Performance Computing at the University of Utah is gratefully acknowledged. The cluster of the Theoretical Division of INR RAS was used for the numerical part of the work.

Appendix A. LDF and shower front fit functions

We perform joint fit of LDF and shower front with 7 free parameters: x_{core} , y_{core} , θ , ϕ , S_{800} , t_0 , a .

$$S(r) = S_{800} \times LDF(r),$$

$$t_0(r) = t_0 + t_{plane} + a \times 0.67 (1 + r/R_L)^{1.5} LDF^{-0.5}(r),$$

where t_{plane} is a shower plane delay, a is a Linsley curvature parameter and the $LDF(r)$ is defined as follows:

$$LDF(r) = f(r)/f(800 \text{ m}),$$

$$f(r) = \left(\frac{r}{R_m}\right)^{-1.2} \left(1 + \frac{r}{R_m}\right)^{-(\eta-1.2)} \left(1 + \frac{r^2}{R_1^2}\right)^{-0.6},$$

$$R_m = 90 \text{ m}, R_1 = 1000 \text{ m}, R_L = 30 \text{ m},$$

$$\eta = 3.97 - 1.79 \times (\sec(\theta) - 1).$$

Appendix B. Smirnov-Cramer-von Mises “omega-square” test implementation

Let $F(x)$ be theoretical distribution and $F_n(x)$ – observed distribution of n events. We define the distance between distributions by [41]:

$$\omega^2 = \int_{-\infty}^{\infty} (F_n(\mathcal{C}) - F(\mathcal{C}))^2 dF(\mathcal{C}).$$

If $\mathcal{C}_1, \mathcal{C}_2, \dots, \mathcal{C}_n$ is a set of observed values in increasing order, ω^2 may be rewritten in the following form:

$$n\omega^2 = \frac{1}{12n} + \sum_{i=1}^n \left(\frac{2i-1}{2n} - F(\mathcal{C}_i)\right)^2.$$

In this paper, we compare the distribution of an event subset with uniform distribution $U(0, 1)$. Therefore $F(\mathcal{C}_i) = \mathcal{C}_i$ and we have:

$$n\omega^2 = \frac{1}{12n} + \sum_{i=1}^n \left(\frac{2i-1}{2n} - \mathcal{C}_i\right)^2.$$

The required maximization of the probability over subsets is therefore reduced to the selection of n different events minimizing the above sum. The latter may be done with a fast iterative procedure.

-
- [1] H. Tokuno *et al.* [Telescope Array Collaboration], J. Phys. Conf. Ser. **293**, 012035 (2011).
 [2] T. Abu-Zayyad *et al.* [Telescope Array Collaboration], Nucl. Instrum. Meth. A **689**, 87 (2012).
 [3] H. Tokuno *et al.* [Telescope Array Collaboration] Nucl. Instrum. Meth. A **676**, 54 (2012).
 [4] M. Ave, J. A. Hinton, R. A. Vazquez, A. A. Watson, E. Zas, Phys. Rev. Lett. **85**, 2244 (2000).
 [5] K. Shinozaki *et al.*, Astrophys. J. **571**, L117 (2002).
 [6] A. V. Glushkov *et al.*, JETP Lett. **85**, 131 (2007).
 [7] A. V. Glushkov *et al.*, Phys. Rev. D **82**, 041101 (2010).
 [8] M. Risse *et al.*, Phys. Rev. Lett. **95**, 171102 (2005).
 [9] G. I. Rubtsov *et al.*, Phys. Rev. D **73**, 063009 (2006).
 [10] J. Abraham *et al.* [Pierre Auger Collaboration], As-

- tropart. Phys. **27**, 155 (2007).
- [11] J. Abraham *et al.* [Pierre Auger Collaboration], *Astropart. Phys.* **29**, 243 (2008).
- [12] M. Settimo, *et al.* [The Pierre Auger Collaboration], *Proceedings of 32nd ICRC, Beijing, 2011*, arXiv:1107.4805.
- [13] V. Berezhinsky, P. Blasi and A. Vilenkin, *Phys. Rev. D* **58**, 103515 (1998).
- [14] K. Greisen, *Phys. Rev. Lett.* **16**, 748 (1966).
- [15] Z. T. Zatsepin and V. A. Kuz'min, *JETP Lett.* **4**, 78 (1966).
- [16] R. U. Abbasi *et al.* [HiRes Collaboration], *Phys. Rev. Lett.* **100**, 101101 (2008).
- [17] J. Abraham *et al.* [Pierre Auger Collaboration], *Phys. Rev. Lett.* **101**, 061101 (2008).
- [18] T. Abu-Zayyad *et al.* [Telescope Array Collaboration], *Astrophys. J. Lett.* **768**, L1 (2013).
- [19] G. B. Gelmini, O. E. Kalashev and D. V. Semikoz, *JCAP* **0711**, 002 (2007).
- [20] D. Hooper, A. M. Taylor and S. Sarkar, *Astropart. Phys.* **34**, 340 (2011).
- [21] S. R. Coleman and S. L. Glashow, *Phys. Rev. D* **59**, 116008 (1999).
- [22] M. Galaverni and G. Sigl, *Phys. Rev. Lett.* **100**, 021102 (2008).
- [23] L. Maccione, S. Liberati and G. Sigl, *Phys. Rev. Lett.* **105**, 021101 (2010).
- [24] G. Rubtsov, P. Satunin and S. Sibiryakov, *Phys. Rev. D* **86**, 085012 (2012).
- [25] P. Satunin, *Phys. Rev. D* **87**, 105015 (2013);
- [26] D. S. Gorbunov *et al.*, *JETP Lett.* **80**, 145 (2004).
- [27] R. U. Abbasi *et al.* [HiRes Collaboration], *Astrophys. J.* **636**, 680 (2006).
- [28] M. Fairbairn, T. Rashba and S. V. Troitsky, *Phys. Rev. D* **84**, 125019 (2011).
- [29] O. E. Kalashev, G. I. Rubtsov, S. V. Troitsky, *Phys. Rev. D* **80**, 103006 (2009).
- [30] D. S. Gorbunov, G. I. Rubtsov and S. V. Troitsky, *Astropart. Phys.* **28**, 28 (2007).
- [31] M. Risse and P. Homola, *Mod. Phys. Lett. A* **22**, 749 (2007).
- [32] L. D. Landau and I. Ya. Pomeranchuk, *Dokl. Acad. Nauk SSSR*, **92**, 535, 735 (1953).
- [33] A. B. Migdal, *Phys. Rev.* **103**, 1811 (1956).
- [34] T. Erber, *Rev. Mod. Phys.* **38**, 626 (1966).
- [35] D. Heck *et al.*, Report FZKA-6019 (1998), Forschungszentrum Karlsruhe.
- [36] W. R. Nelson, H. Hirayama, D.W.O. Rogers, SLAC-0265.
- [37] P. Homola *et al.*, *Comp. Phys. Comm.* **173** 71 (2005).
- [38] B. T. Stokes *et al.*, *Astropart. Phys.* **35**, 759 (2012).
- [39] S. Agostinelli *et al.* [GEANT4 Collaboration], *Nucl. Instrum. Meth. A* **506**, 250 (2003).
- [40] B. Stokes *et al.* "Using CORSIKA to quantify Telescope Array surface detector response" *Proceedings of the 31th ICRC in Lodz* (2009).
- [41] E. L. Lehmann, J. P. Romano, *Testing Statistical Hypotheses*, Springer, 2010.
- [42] J. Alvarez-Muñiz *et al.* "Review of the Multimessenger Working Group at UHECR-2012" *Proceedings of UHECR 2012 Symposium, CERN* (2012).
- [43] Due to limited MC statistics \mathcal{C} distribution for photon MC events differ from uniform. The deviations do not exceed 5%, see Figure 4.